

# Quantitative Assessment of Drought Severity in Mining-Influenced Regions: A Case Study of Lignite and Copper Extraction Areas

Zofia Rzepecka , Monika Birylo\* 

University of Warmia and Mazury in Olsztyn, Faculty of Geoengineering, Olsztyn, Poland

\* Corresponding author

**Abstract:** Droughts occurring in open-pit mining areas are becoming increasingly significant, primarily due to decreased water availability. This poses a danger because it threatens the stable development of society and agricultural production and contributes to increased dust emissions that may interfere with mining operations. Climate change further intensifies these threats. Therefore, research into water availability, continuous monitoring, and environmental health indicators is vital, as the water cycle greatly impacts these factors. The paper aims to investigate drought severity in two large open-pit lignite mines in Turów and Bełchatów, and Legnica–Głogów Copper District (LGOM). The Combined Climatological Drought Index (CCDI) was used, alongside the water budget (WB), to characterise drought at the study sites. High consistency between the indices was observed throughout most of the studied period until 2018. Notably, significant reductions in water availability were recorded from 2018 onwards in the areas of the three studied mines.

**Keywords:** drought severity, GLDAS, CCDI, water budget, groundwater

Received: January 20, 2026; accepted: April 7, 2026

© 2026 Author(s). This is an open-access publication that can be used, distributed, and reproduced in any medium according to the Creative Commons Attribution 4.0 International License (CC BY 4.0).

---

E-mails & ORCID iDs: [zofia.rzepecka@uwm.edu.pl](mailto:zofia.rzepecka@uwm.edu.pl), <https://orcid.org/0000-0002-6570-9032> (Z.R.);  
[monika.sienkiewicz@uwm.edu.pl](mailto:monika.sienkiewicz@uwm.edu.pl), <https://orcid.org/0000-0002-8006-288X> (M.B.).

## 1. Introduction

In the context of climate change, extreme events are becoming more frequent and intense. Such phenomena include floods and droughts. An additional aspect, apart from climate change, is human activity, especially the intensive disturbance of the subsurface structure. In particular, open-pit mines warrant special attention, where evaporation is reduced, subsurface pathways for groundwater flow are disrupted, and artificial drainage is introduced. Such mines occupy large areas, hence the need for continuous monitoring, especially of fluctuations and declines in groundwater levels. For assessing drought sensitivity, the Combined Climatological Drought Index (CCDI) is an effective tool.

Drought, which is occurring more frequently, threatens both ecosystems and societal functioning. Therefore, its quantification is extremely important. Hydrological and meteorological data can be used to assess drought conditions.

Research on groundwater and water balance in the context of mines is crucial because the exploitation of raw materials can significantly affect local hydrological conditions. Open-pit mines alter the natural water cycle and may also lead to declines in groundwater levels, changes in water quality, or increased flood risk. This is of crucial importance, as access to water is fundamental to environmental balance and ensuring sustainable development. Lian et al. [1] studied the vadose zone in open-pit mining areas and noted that open-pit mining operations resulted in a decrease in soil moisture by approximately 15%, and groundwater levels decreased by an average of approximately 0.2 m per year. Haque et al. [2] studied an open-pit coal mine and its impact on groundwater resources in and around the mine. This is particularly important in the Phulbari area in Dinajpur District, as groundwater is the primary source of water for agriculture and domestic use.

On the other hand, deep mines are also worth investigating, as the extraction of large volumes of ore from underground has significant impacts on water conditions, including rock mass movement, paraseismic tremors, drainage of Tertiary layers, sometimes extending several dozen kilometres from the mine.

Mines, both open-pit and underground, cause significant, often irreversible, groundwater losses through rock mass drainage processes. Raw material extraction lowers the groundwater table, resulting in the formation of cones of depression, drying out wells and rivers, and the degradation of ecosystems. Mining operations, especially in open-pit lignite mines, require intensive dewatering of the deposit to prevent flooding of the excavations. Prolonged groundwater pumping creates a cone-shaped depression, which can extend across tens or even hundreds of square kilometres. Lowering the groundwater table directly causes wells to dry out [3, 4]. The aim of the study was to confirm that mines generate groundwater losses. In this study, we consider mine drainage to be one of the main causes of water resource degradation; therefore, groundwater levels and drainage parameters were analysed in the mines under study.

In recent years, research on the impact of mining activities on changes in water conditions in the surrounding area has become particularly important in Poland. The Turów mine lies near the borders of three countries: Poland, the Czech Republic, and Germany. In the public spheres of these three countries, as well as in the European Union, discussions about the declining groundwater levels in the Turów area, which affect all three countries, have been ongoing [5, 6].

In the Legnica–Głogów Copper District, research into the environmental impact of mining began simultaneously with the construction of the first mines. Research on water conditions is particularly important because during ore extraction, permanent drainage of the rock mass is carried out. This leads to drying of the area and subsidence of the ground surface, which is reflected in the formation of a large surface trough. The subsidence is continuously observed using precise geodetic methods (GNSS surveys, precise levelling) [7–9].

The paper aimed to assess drought severity in two Polish open-pit lignite mines (Turów and Bełchatów) and one underground copper mine in the Legnica–Głogów Copper District (LGOM). The research is based on the assessment of selected hydrological parameters (CCDI and WB) and on trends derived from the Mann–Kendall method.

## 2. Mines Selected for Research

The article analyses grid cells corresponding to three mines located in Poland:

- Turów open-pit lignite mine;
- Bełchatów open-pit lignite mine;
- Legnica–Głogów Copper District (Polish: Legnicko-Głogowski Okręg Miedziowy, LGOM) – a complex of deep mines extracting mainly copper, with smaller amounts of silver and rock salt.

The locations of the three mines, together with the centres of the grid cells for which all data was collected, are shown in Figures 1–3.

The **Turów mine** is located in Eastern Upper Lusatia (Czech: Žitavská pánev, German: Östliche Oberlausitz, Polish: Obniżenie Żytawsko-Zgorzeleckie), situated between the Lusatian Massif and the western part of the Iżera Mountains, in the Iżera Foreland, near the town of Turosszów. The Turosszów deposit is located at  $\varphi = 50.833\text{--}50.875^\circ$  N and  $\lambda = 14.850\text{--}15.000^\circ$  E. The mine is in the western part of the Dolnośląskie Voivodship, in the central part of the so-called Turosszów Coal Basin, lying between the state borders of Germany and the Czech Republic. This mine began industrial lignite extraction using the open-pit method as early as 1904, initially under the name Herkules. In 1947, the exploited deposit was named Turów I. In 1968, construction of the Turów II mine began. At that time, a power plant was also established in the nearby town of Turosszów [10].

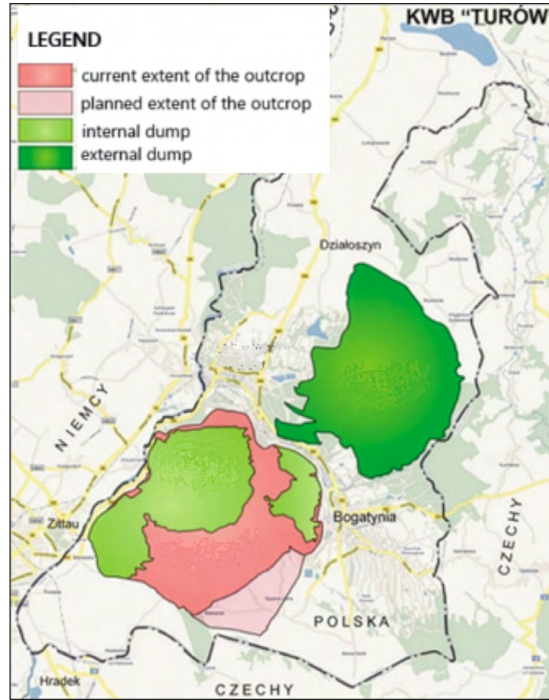


Fig. 1. Turów mine complex area

Source: [11], modified

Annual production is around 12 million tonnes of lignite; additionally, 30 million m<sup>3</sup> of overburden is removed. The surface of the open pit is 2,400 ha. The excavation reaches a depth of 300 m and covers around 30 km<sup>2</sup>. Lignite, the primary fuel, is delivered by belt conveyors to the Turów Power Plant.

The **Bełchatów open-pit lignite mine** started its operations in 1980 [12].

The mine area is located in the Southern Mazovian Hills, in the Bełchatów Upland mesoregion on the Rakówka River, approximately 50 km south of Łódź and approximately 25 km west of Piotrków Trybunalski. The approximate coordinates of the mine are  $\varphi = 51.224^\circ$ ,  $\lambda = 19.406^\circ$ .

The entire Bełchatów lignite complex stretches for about 30 km from east to west and 5 km from north to south (Fig. 2). It includes a power plant, two open-pit lignite fields (Bełchatów and Szczerców) and a dump of overburden extracted during mining operations. The excavations reach a depth of 200 m and are among the largest “holes in the ground” in Europe. Two mountains were built from the soil extracted from the excavation: Kamięńsk Mountain and the newly created external dump of the Szczerców field. At 406 m above sea level, Kamięńsk Mountain is the highest elevation in central Poland. This mountain has undergone full land reclamation and afforestation, as waste storage there was completed in 1993 [13].

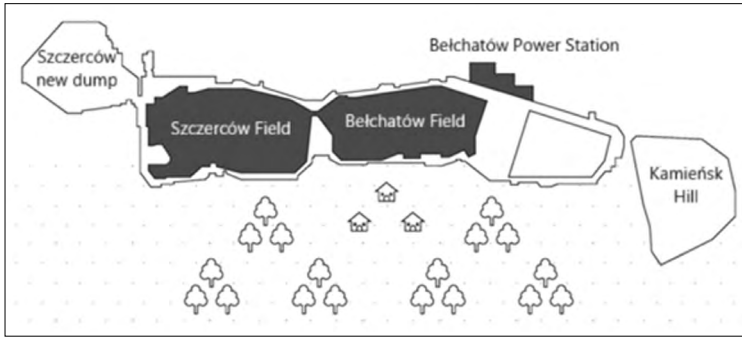


Fig. 2. Bełchatów lignite open-pit mine complex

Source: [14], modified

In recent years, the Bełchatów mine has produced around 40–42 million tonnes, accounting for over 60% of Poland's total lignite production. To achieve such results, an average of over 120 million m<sup>3</sup> of overburden must be removed annually, and around 270 million m<sup>3</sup> of water must be pumped out [13].

It is predicted that most of Poland's lignite and hard coal-fired power plants will become unprofitable by 2031 due to high fuel costs and rising EU CO<sub>2</sub> emission prices. For Bełchatów, the oldest units are expected to become unprofitable before 2030, as capacity market payments supporting the plant are due to end in 2028 [12].

The **Legnica–Głogów Copper District (LGOM)** is located in southwestern Poland, within the Fore-Sudetic Monocline (Fig. 3). It covers an area of about 400 km<sup>2</sup> [3]. The approximate coordinates of the centre of the mining area are  $\varphi = 51.504^\circ$ ,  $\lambda = 16.073^\circ$ .

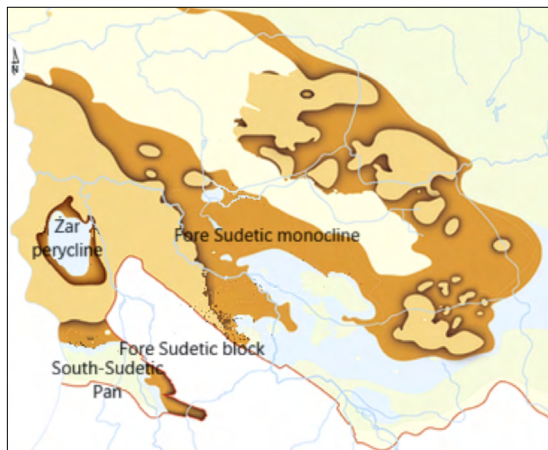


Fig. 3. The distribution of copper ore deposits in Poland

Source: own elaboration according to [16]

Research conducted in Poland in the 1950s led to the discovery in 1957 of rich but deeply situated copper deposits between Legnica and Głogów. LGOM began to develop in 1960; in 1968, the Lubin and Polkowice mines were launched, followed by Rudna in 1974 and Sieroszowice after 1978 [15]. Currently operating mines are marked in Figure 3.

In Poland, copper is extracted exclusively in deep mines. In the LGOM mines, extraction is carried out at depths of 600 to 1,250 m, producing about 30 million tonnes of ore per year with an average copper content of about 1.6% and 45 g of silver per tonne [17]. Current exploitation systems are given and analysed in [8], and can be summarised as follows:

- chamber pillar system with additional protection of the roof (R-UO);
- two-layer chamber pillar system with hydraulic filling (RG-5);
- picking of the deposit based on the splitting of the one-stage chamber pillar system with hydraulic filling;
- two-stage picking of the deposit, in the resistance pillar of the excavations.

The system R-UO is currently the most commonly used. It is applied to deposits up to 7 m thick.

Over the past 50 years, Poland has produced 18 million tonnes of copper (and mined over a billion tonnes of ore). Current copper resources allow for continued mining for another 50 years. The balance of resources in 2015 in the Fore-Sudetic Monocline and North-Sudetic Basin regions totalled 1,976 million tonnes of ore containing 36 million tonnes of copper. For example, in 2015, copper ore mining amounted to 32 million tonnes of ore with a Cu content of 1.52%, containing 479 thousand tonnes of copper.

Such high copper extraction rates cause significant impacts in the surrounding areas. These impacts can be divided into direct (caused by the movement of the rock mass into the post-mining void), dynamic (resulting in paraseismic tremors) and indirect (related to the drainage of Tertiary layers, appearing on the surface in the form of large-area subsidence (drainage basin)). All three types of impacts may cause changes in water conditions across a large area surrounding the mine (see e.g. [9]).

### 3. Data and Its Characteristics

Selected GLDAS (Global Land Data Assimilation System) products were used in this study. GLDAS is a system that provides high-resolution geoscience data for the Earth's land surface. The model is based on many sources of observations, including satellite, airborne, and ground-based observations, as well as modelling outputs. Thanks to GLDAS, it is possible to analyse how the land surface interacts with the atmosphere [18]. Currently, GLDAS consists of four sub-models: Mosaic,

NOAH, VIC, and CLM. Among them, the GLDAS CLSM product has a 1-month resolution of  $0.25^\circ \times 0.25^\circ$ , making it desirable for hydrological cycle studies [19]. From the dataset used in this study, the following data were collected from the CLSM GLDAS model: evapotranspiration, surface, and subsurface runoff, and groundwater [20]. As precipitation could not be obtained from the model, it was downloaded from NOAH [21].

Precipitation is any form of water that falls to the ground and feeds the water system; thus, it is a basic element of the hydrological system, constituting the most significant component of the WB [22]. It also shapes climatic conditions. Water feeds the hydrological system in various forms. Evapotranspiration combines two phenomena: evaporation and plant transpiration. This process represents water loss from the land surface. Evaporation is the escape of water in the form of water vapour from surface waters (e.g. lakes, rivers) and other water bodies. Transpiration results from plant metabolism (including photosynthesis).

Evapotranspiration plays an important role in the water budget as it determines the availability of water in the soil and the regional climate [23]. Surface runoff is the movement of water that has not been absorbed into the soil and does not evaporate, but instead flows along the land surface, reaching river basins or reservoirs. The phenomenon has a significant impact on river formation and flood occurrence. Surface runoff occurs when precipitation exceeds infiltration capacity, which is influenced by soil saturation, soil type, land cover, or slope. The speed of surface runoff is influenced by the intensity and duration of rainfall [24]. Groundwater, in the context of the GLDAS model, is one of the key hydrological variables modelled by this system. In GLDAS, groundwater is calculated as the difference between total water storage and the sum of soil moisture, snow water equivalent, canopy water, and surface water storage. GLDAS considers various hydrological processes that influence water movement through the soil, including infiltration, soil water movement, groundwater recharge, and groundwater flow [22].

To investigate the impact of mining activities in the three selected mines on the surrounding terrain, the time series behaviour of six selected quantities was analysed:

- total water storage (TWS) – obtained from GRACE observation processing, expressed in millimetres of equivalent water height;
- groundwater storage (GWS) – obtained from the CLSM model, calculated as GRACE TWS minus root zone soil moisture, also expressed in millimetres;
- surface runoff ( $Q_s$ ) – obtained from the CLSM model, a dynamic variable expressed in millimetres per second, it represents the rate of change of surface water storage, due to surface runoff;
- subsurface runoff ( $Q_{sb}$ ) – also obtained from the CLSM model as a dynamic variable, representing the rate of change of subsurface water storage, expressed in millimetres per second; indicating changes in subsurface water storage over time;

- precipitation rate (P) – obtained from the NOAA model, its value is given in millimetres per second, and is therefore a dynamic variable showing variations in equivalent water height due to any kind of precipitation;
- evapotranspiration (EV) – total evapotranspiration rate, obtained from the CLSM model; a dynamic variable expressed in millimetres per second, representing water loss through evaporation and transpiration from the canopy, soil, and snow.

The time series of the above values was examined for the period from February 2003 to February 2024 (253 monthly observations). The values for the cells containing the selected mines were compared with those of the remaining cells in the study area. The area extends between the geographic coordinates defined as  $\lambda \in (14^\circ, 24^\circ)$  and  $\varphi \in (49^\circ, 55^\circ)$  (see Fig. 4). A spatial resolution of  $0.25^\circ$  over this area results in 1,125 cells being included in the analysis.

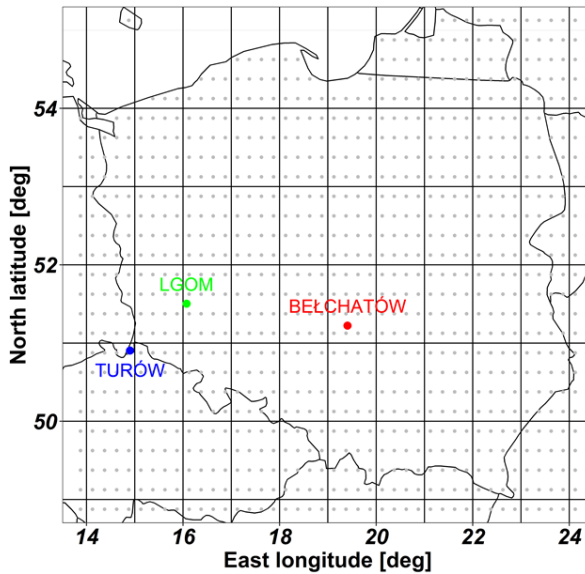


Fig. 4. Research area, data resolution and location of three mines included in the analysis

Basic statistics for the downloaded data are shown in Table 1, and the trends in selected variables over time are shown in Figure 5.

Rows 1–3 present the mean values over time for the grid cells corresponding to the three analysed mines. Rows 4–6 show the range (maximum, minimum, and overall mean) of time-averaged values calculated for all 1,125 grid cells. Rows 7–9 present the spatial statistics (maximum, minimum, and overall mean) calculated across all cells at each time step. Rows 10–11 provide the absolute maximum and minimum values of each variable observed across all cells and all time steps. Further details are provided in the Appendix.

**Table 1.** Basic statistics of the variables included in the analysis

No.	Statistic parameter	TWS [mm]	GWS [mm]	Qs [mm/s]	Qsb [mm/s]	P [mm/s]	EV [mm/s]
1	Mean over time (Bełchatów)	670.94	521.17	1.13e-07	1.64e-06	2.31e-05	1.49e-05
2	Mean over time (LGOM)	616.56	481.04	2.74e-08	2.06e-06	2.50e-05	1.40e-05
3	Mean over time (Turów)	1,155.18	885.77	1.46e-07	2.46e-06	2.65e-05	1.85e-05
4	Mean over time (max)	2,464.64	2,072.45	2.29e-06	8.56e-06	3.53e-05	2.67e-05
5	Mean over time (min)	537.27	406.72	0e0	3.05e-07	1.95e-05	1.22e-05
6	Mean over time (overall)	1,119.19	879.39	8.50e-08	1.77e-06	2.49e-05	1.68e-05
7	Mean over cells (max)	1,287.12	1,016.97	2.79e-07	1.32e-05	6.75e-05	5.82e-05
8	Mean over cells (min)	971.82	761.22	1.57e-08	0e0	2.65e-06	-2.02e-06
9	Mean over cells (overall)	1,119.19	879.39	8.50e-08	1.77e-06	2.49e-05	1.68e-05
10	Max value	2,585.37	2,142.60	7.77e-06	0e0	1.02e-04	1.29e-04
11	Min value	384.94	294.27	0e0	0e0	1.25e-08	-1.04e-04

Notes: TWS – total water storage, GWS – groundwater storage, Qs – surface runoff amount, Qsb – subsurface runoff amount, P – precipitation, EV – evapotranspiration.

Only TWS and GWS are static variables, expressed as equivalent water column heights (in millimetres). They represent the water content of a given area at a given moment. The remaining variables are dynamic and expressed as rates of change of equivalent water column height (in millimetres per second). TWS and GWS exhibit clear seasonal variability, with amplitudes on the order of 200 mm. The mean TWS values for the Bełchatów, LGOM, and Turów areas are approximately 670, 616, and 1,155 mm, respectively, with the highest values observed in Turów. A similar pattern is observed for GWS, with corresponding mean values of approximately 520, 480, and over 880 mm. Across the entire study area, TWS and GWS values range approximately from 540 (410) to 2,465 (2,070) mm. The values for Turów lie near the centre of this range, whereas those for Bełchatów and LGOM are closer to the lower bound. Therefore, the obtained time series of TWS and GWS for Turów closely resemble the spatial average across all 1,125 cells. In general, the average TWS and GWS values are the lowest in central Poland, where the Bełchatów and LGOM mines are located.

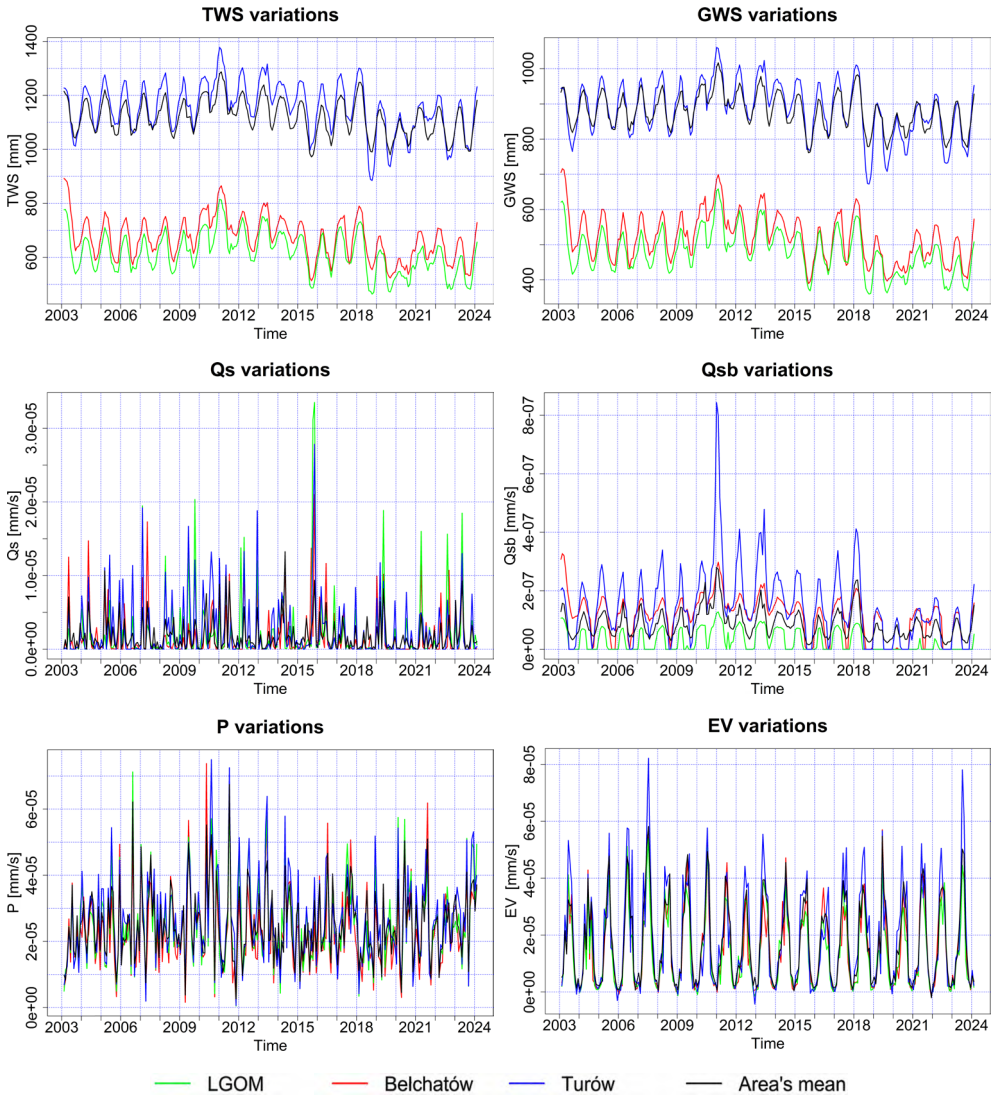


**Fig. 5.** Time series of the input data for the cells containing the selected mines.  
Notes: TWS – total water storage, GWS – groundwater storage, Qs – surface runoff, Qsb – subsurface runoff, P – precipitation, EV – evapotranspiration

Dynamic variables have much smaller magnitudes, as they are expressed in millimetres per second. To obtain approximate monthly changes, these values can be multiplied by the average number of seconds in a month (i.e.,  $365.25 \cdot 86,400/12 = 2,629,800 \approx 2.63 \cdot 10^6$  s).

Table 1 contains the original data obtained from the GLDAS model. Based on these data, approximate values of water content changes in mm per month are

provided here, as these units are more intuitive. In these units, the mean surface runoff ( $Q_s$ ) in the study area ranges from 0 to 6 mm per month, and for the Bełchatów, LGOM, and Turów cells, these values are 0.3 mm, 0.1 mm and 0.4 mm, respectively. These values are small and near the lower bound, though they are highest for Turów. The values of monthly changes caused by subsurface runoff ( $Q_{sb}$ ) are generally larger; in the study area, they range from 0.8 to 22.5 mm, whereas the values calculated for the mine cells are 4.3, 5.4, and 6.5 mm, respectively. Again, these values are closer to the minimum. The situation is similar for evapotranspiration (EV), with monthly values of 39.2 mm/s, 36.8 mm/s, and 48.6 mm/s for Bełchatów, LGOM and Turów, and the range for the entire area is 32.1–70.2 mm per month. Monthly changes in water content caused by precipitation for cells containing the mines are 60.7, 65.7 and 69.7 mm, and the minimum and maximum for all cells are 51.3 and 92.8 mm. It should be noted that mining activities can affect runoff (both surface and subsurface) and evaporation; however, they are not expected to directly influence precipitation. Precipitation is included here because it is a component of the indicators used to assess changes in water conditions in the analysed areas. Additionally, it should be emphasised that among the dynamic variables, only precipitation represents water input to the system, whereas the remaining variables represent water losses from the system.

#### 4. Methodology

The paper aims to determine parameters describing and characterising drought. For this purpose, the Combined Climatologic Drought Index (CCDI) and the water budget (WB) were computed. The steps of the research are presented in the flowchart (Fig. 6). Determining these parameters enables the evaluation of hydroclimatic extreme events, assessment of spatiotemporal patterns, drought impacts, and the applicability of GRACE and GLDAS-derived models [25].

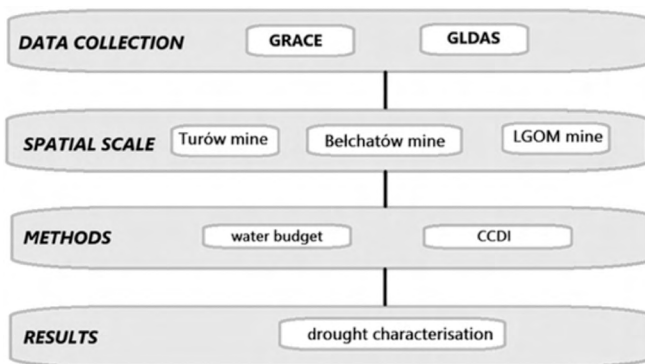


Fig. 6. Flowchart presenting the steps of analysis

Drought conditions in the lignite and copper mining areas are characterised by using two types of data: terrestrial and atmospheric water. For this purpose, precipitation anomaly (PA) and total water storage anomaly (TWSA) were used. PA was calculated as follows [26, 27]:

$$PA = P - \bar{P} \tag{1}$$

where: PA is a precipitation anomaly time series, P is a precipitation time series, and  $\bar{P}$  is the mean monthly precipitation.

Residuals for both precipitation and total water storage were then determined [26, 27]:

$$PA^R = PA - \overline{PA} \text{ and } TWSA^R = TWSA - \overline{TWSA} \tag{2}$$

where:  $PA^R$  and  $TWSA^R$  denote residual time series,  $\overline{PA}$  and  $\overline{TWSA}$  denote their respective mean values.

The residual deviation  $CD^R$  is defined as the sum of  $PA^R$  and  $TWSA^R$  residuals [15, 16]:

$$CD^R = PA^R + TWSA^R \tag{3}$$

Having computed  $CD^R$ , the CCDI time series can be defined as follows [26, 27]:

$$CCDI = \frac{CD^R - \overline{CD}}{\sigma(CD^R)} \tag{4}$$

where  $\overline{CD}$  denotes the mean of  $CD^R$  and  $\sigma(CD^R)$  denotes its standard deviation.

The drought severity index can be classified by grouping values into categories defined by the CCDI scale (Table 2) [27].

**Table 2.** Drought severity classification based on CCDI

Level	Category	CCDI
W4	extremely wet	(1.45; ∞)
W3	severely wet	(0.94, 1.44]
W2	moderately wet	(0.46, 0.93]
W1	mildly wet	(0.28, 0.45]
N0	normal	(-0.28, 0.29]
D1	mild drought	(-0.44, -0.29]
D2	moderate drought	(-0.93, -0.45]
D3	severe drought	(-1.44, -0.94]
D4	extreme drought	(-∞, -1.45]

The next part of the study involved comparing the results with groundwater storage anomalies (GWSA using well measurements provided by the National Hydrogeological Service of Poland and satellite data from GRACE and GLDAS, calculated as follows [28]:

$$\text{GWSA} = \text{TWSA} - \text{SMA} - \text{SWEA} - \text{SWSA} \quad (5)$$

where SMA, SWEA, and SWSA denote soil moisture, snow water equivalent, and surface water storage anomaly time series, respectively.

A basic hydrological quantity is the water budget (WB). It is often used for assessing the amount of water in a system. WB is defined as the difference between water inputs and outputs. Thus, it represents the balance between precipitation, evapotranspiration, and surface runoff [29, 30]:

$$\text{WB} = \text{P} - \text{EV} - \text{Qs} - \text{Qsb} \quad (6)$$

where P is the precipitation time series, EV is the evapotranspiration time series, Qs is the surface runoff time series, and Qsb is the subsurface runoff time series.

The analysis was carried out using four sets of values: TWS, GWS, CCDI and WB. TWS and GWS were obtained directly from online data sources (see Section 3), while CCDI and WB were calculated:

- CCDI was calculated according to Equation (4) and represents a standardised index that facilitates the determination of soil moisture conditions, ranging from extremely wet through normal to extreme drought (see Table 2).
- WB was calculated according to Equation (6), where evapotranspiration (EV) and surface and subsurface runoff (Qs and Qsb) were taken from the CLSM model, and precipitation (P) from the NOAH model. All variables are expressed in millimetres per second and represent rates of change in water content. WB values are positive when water inputs exceed outputs and negative otherwise.

Mean values and linear trends were calculated for all cells in the study area, and their statistical significance was assessed using the Mann–Kendall test.

Trends were estimated by fitting the following model:

$$y = a_0 + a_1 t + a_2 \sin(\omega t) + a_3 \cos(\omega t) \quad (7)$$

where the coefficients  $a_i$ ,  $i = 0, \dots, 3$ , are computed by minimising the residuals of the fitting. The coefficient represents the linear slope of the fitted data. In our case, the trend results obtained from the original data have the following units: millimetres per day [mm/day] for TWS and GWS, millimetres per second per day [mm/s/day] for Qs, Qsb, and WB, and one per day [1/day] for CCDI data.

To assess whether the trend computed is statistically significant, the Mann–Kendall test (MK test) was applied. This non-parametric test evaluates whether a time

series exhibits a monotonic trend by analysing the signs of differences between successive observations [31]. Due to seasonality, the seasonal Mann–Kendall test was applied [32]. Statistical significance was evaluated using a  $p$ -value threshold of 0.05.

## 5. Results

As mentioned in Section 4, the focus was on examining the time series behaviour of six selected quantities: TWS, GWS,  $Q_s$ ,  $Q_{sb}$ , CCDI, and WB. The first four variables were taken directly from the GLDAS system and presented in Section 3 (Fig. 5, Table 1). The remaining two values were calculated based on the input data (see Section 4). Their brief characteristics are given below (Fig. 7, Table 3).

Figure 7 presents the time series of the aforementioned variables for cells containing selected mines (Fig. 4) and the mean values of a given variable calculated over the entire area (comprising 1,125 cells).

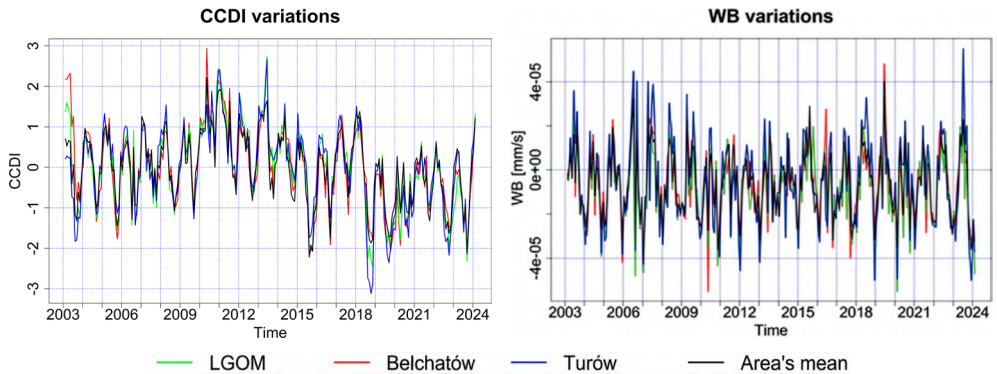


**Fig. 7.** Time series of WB and CCDI for grid cells containing selected mines, together with mean values of a given variable calculated for the entire area (containing 1,125 grid cells)

Numerical values of the means and ranges are presented in Table 3.

The results indicate that the mean values for the grid cells containing the mines fall between the minimum and maximum values observed across the entire area, for both WB and CCDI. The mean values for the entire area (1,125 grid cells) do not differ significantly from those obtained for the grid cells containing the selected mines. The calculated CCDI values (see Equation (4)) range from about  $-3$  to  $+3$ ; they are dimensionless and indicate the degree of soil moisture. In the study area, the means are close to zero, indicating normal soil moisture conditions (see Table 2). However, at the end of 2018, a marked decrease in this index was recorded across the entire area, indicating a temporary extreme drought. WB values (calculated according to Equation (6)) range between  $-5$  and  $5$  mm/s, but in the 2012–2018 period, the amplitude decreases to between  $-2.5$  and  $2.5$  mm/s. The highest values regularly occur in summer, and the lowest in winter.

**Table 3.** Basic statistics of the quantities studied

Statistics description	WB [mm/s]	CCDI
Mean over time (Bełchatów)	-6.51e-06	3.48e-16
Mean over time (LGOM)	-8.90e-06	6.97e-16
Mean over time (Turów)	-5.45e-06	9.14e-16
Mean over time (max)	5.42e-06	3.54e-15
Mean over time (min)	-1.46e-05	-3.61e-15
Mean over time (overall)	-6.21e-06	2.17e-17
Mean over cells (max)	4.12e-05	2.21
Mean over cells (min)	-4.01e-05	-2.20
Mean over cells (overall)	-6.21e-06	2.53e-17
Max value	-8.17e-05	4.06
Min value	-2.28e-04	-3.48

To assess the influence of mining activities on water conditions, trends in the variables of interest were analysed. Linear trends of the studied variables were calculated, and their statistical significance was assessed using the seasonal Mann-Kendall test (see Section 4).

The research results are presented in Figures 8–10 (selected grid cells) and Figure 11 (the entire area), while precise numbers are provided in Table 4.

**Table 4.** Linear trend values for Bełchatów, LGOM and Turów cells together with minimum and maximum trend values for the entire study area

Trend description	Bełchatów	LGOM	Turów	Min. trend	Max. trend
TWS trend [mm/day]	-0.0132	-0.0111	-0.0119	-0.0261	0.01592
TWS trend [mm/year]	-4.8162	-4.0578	-4.3641	-9.5489	5.8148
GWS trend [mm/day]	-0.0113	-0.0092	-0.0099	-0.0212	0.0126
GWS trend [mm/year]	-4.1277	-3.3736	-3.6379	-7.7625	4.6043
WB trend [mm/s/day]	-2.22e-10	-2.83e-10	-2.44e-10	-8.66e-10	1.19e-09
WB trend [mm/s/year]	-8.12e-08	-1.03e-07	-8.92e-08	-3.16e-07	4.35e-07
CCDI trend [1/day]	-0.0002	-0.0001	-0.0001	-0.0003	0.0002
CCDI trend [1/year]	-0.0566	-0.0491	-0.0429	-0.0963	0.0611

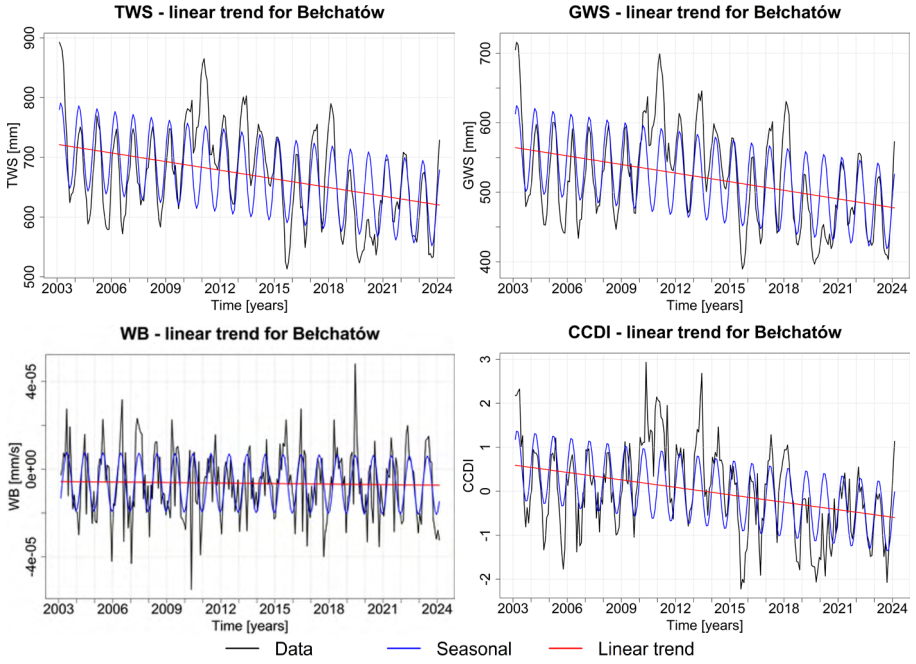


Fig. 8. Water condition indicators (TWS, GWS, WB and CCDI) for the cell of Bełchatów

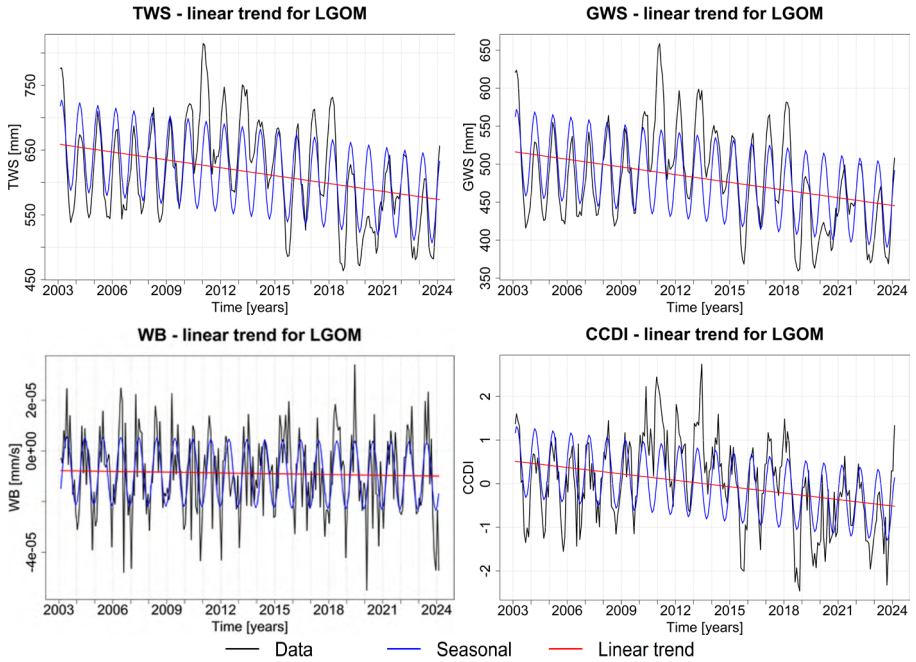
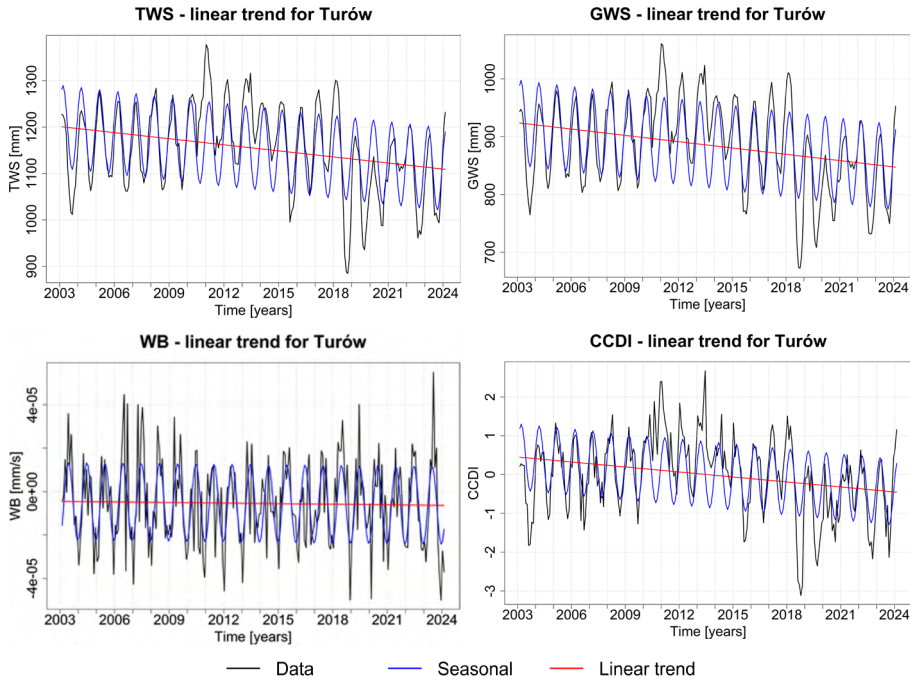


Fig. 9. Water condition indicators (TWS, GWS, WB and CCDI) for the LGOM cells



**Fig. 10.** Water condition indicators (TWS, GWS, WB and CCDI) for the Turów cell

The calculated CCDI values enable the characterisation of drought conditions and their temporal occurrence. All D4–W4 categories were observed across the study area throughout the study period.

In the years 2003–2009, each time series moved regularly between minimum and maximum values with the seasons, reaching the D3 (severe drought) limit at the minima and the W3 (severe wet) limit at the maxima. Double peaks were observed during this period.

From late 2009 to 2015, CCDI values became increasingly inconsistent, with multiple peaks occurring each year. The lowest values in these years decreased to D1 (mild drought) or slightly exceeded D2 (moderate drought), reaching twice that level. In each year, the highest values reached W4 (extremely wet) levels, sometimes twice within a single year (2010 and 2011).

Between 2015 and 2018, seasonal variability stabilised again across all study locations; however, the amplitude of fluctuations increased compared with the earlier period (D4–W4). This increase also progressed from year to year. In autumn 2017, Turów and LGOM reached the N0 (normal) minimum, whereas in Bełchatów, the minimum reached D3 (severe drought). In 2018, the minimum value in Bełchatów occurred 2 months earlier than in Turów and LGOM, and reached D2 (moderate drought), while the other two mines reached D3 (severe drought).

At the turn of 2018–2019, there was a marked drop in values, resulting in D4 (extreme drought). The Bełchatów mine area barely exceeded the D4 threshold, LGOM showed intermediate values, and Turów experienced a dramatic drop. Then, until 2021, persistent drought conditions were observed, rarely reaching N0. Seasonal regularity is reduced during this period, with two peaks and two troughs.

From the end of 2021, moderate regularity returned, but this period can still be classified as dry, as the maximum values remained within W1 (mild wet), or sometimes barely exceeding the level of W2 (moderately wet), while the minimum values reached D2 (moderate drought) in 2021, D4 (extreme drought) in 2022, 2023 and 2024.

Based on Table 4 and Figure 11, clear decreasing trends are observed for TWS, GWS, and CCDI across both mine cells and most of the study area. This indicates a decline in average water availability. No clear differences are observed between mine cells and the surrounding area. For TWS, the calculated trends range from  $-9.5$  to  $5.8$  mm/year, and for mine cells, the corresponding values range from  $-4.8$  to  $-4.0$  mm/year. These values lie approximately midway between the minimum and maximum observed across the study area. Analogous values for GWS range from  $-7.8$  to  $4.6$  mm/year (minimum/maximum) and from  $-4.1$  to  $-3.3$  mm/year (mine cells).

Similarly, the trends for WB and CCDI fall within the overall range of minimum and maximum values observed across the study area, indicating both lower and higher rates of change. Regarding the statistical verification of trends using the Mann–Kendall test, the behaviour of WB differs from that of the other variables. For TWS, GWS and CCDI, the calculated positive trends are statistically significant across most cells, while the negative trends are generally not statistically significant (high  $p$ -values). In the case of WB, however, neither the calculated positive nor negative trends pass the test in most cases, which indicates that the trend is weak and the estimates are unreliable.

Figure 8 shows an analysis of the linear trend, seasonality, and CCDI for Bełchatów. The linear trend has a negative slope, meaning that CCDI decreased between 2003 and 2023, indicating a long-term downward trend. Thus, regardless of seasonal fluctuations, the average CCDI level is systematically decreasing. Similarly, clear cyclical behaviour is observed, with a strong seasonal component. High variability was observed between 2003 and 2013, with periods of high values. After 2015, values below zero became increasingly frequent, and the amplitude of fluctuations decreased.

Long-term decline in CCDI values can be observed in Bełchatów. The reduction in amplitude after 2015 may indicate stabilisation or weakening of seasonal factors. In the studied open-pit mine area, CCDI values may reflect climatic or environmental conditions, particularly changes in moisture levels. These patterns may be associated with industrial activity influencing the microclimate. It can also be observed that the average CCDI is decreasing, indicating a shift relative to previously observed conditions.

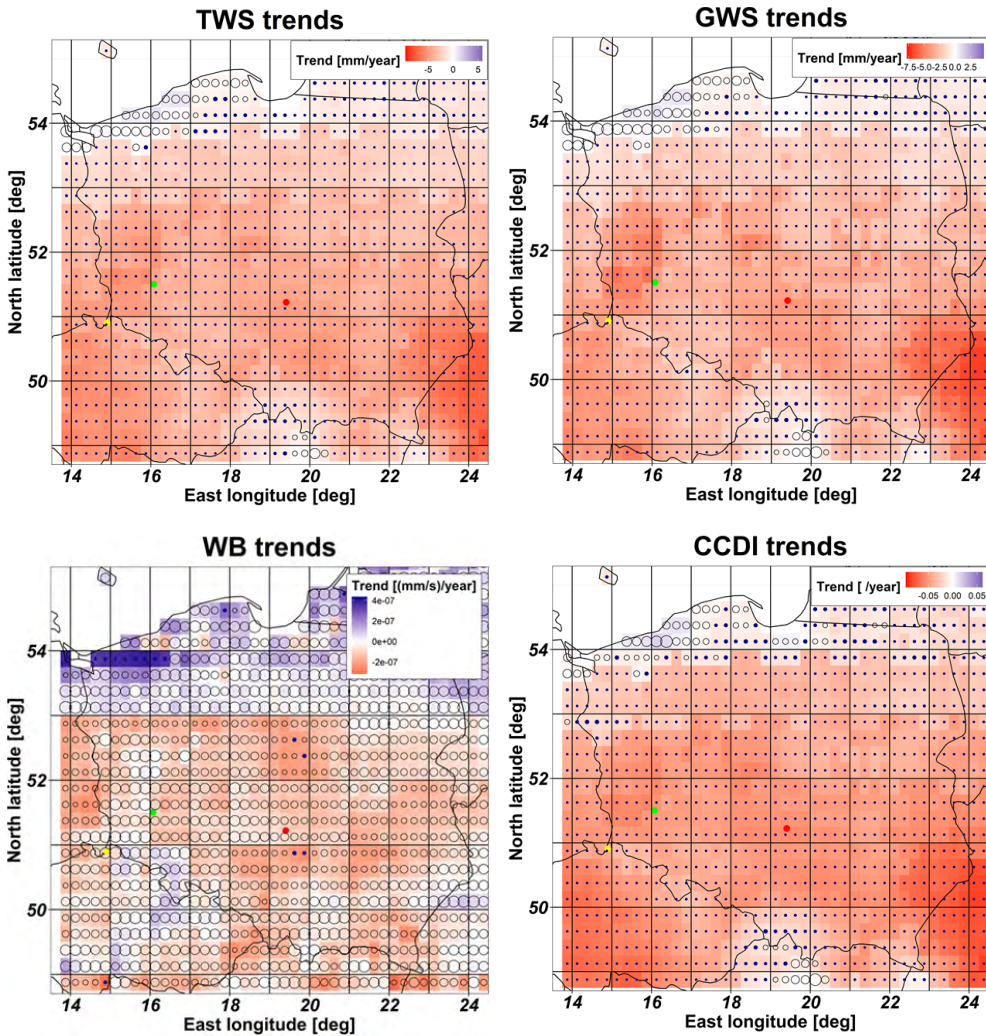


**Fig. 11.** Calculated trends and results of the Mann–Kendall test. Colours correspond to the calculated trends for individual cells, as shown in the legends. The size of the markers is proportional to the  $p$ -value from the MK test. A filled marker (dot) indicates a statistically significant trend, whereas an unfilled marker (empty circle) indicates a non-significant trend

The trend line has a negative slope (Fig. 9), indicating that CCDI values declined between 2003 and 2023. The decline is moderate but sustained over the study period. Strong, regular annual fluctuations are observed, with a clear rhythm, as values alternate between increases and decreases. Compared to Bełchatów, the trend is negative in both locations, but in the LGOM region, the seasonal amplitude remains more stable throughout the period; extreme fluctuations are less pronounced than

in Bełchatów. This suggests that conditions in the LGOM region are more stable and less susceptible to abrupt changes. As for the CCDI, fluctuations have decreased in recent years (after 2018), which may indicate stabilisation of climatic conditions.

Based on Figure 10, the CCDI values in Turów steadily decreased over the 2003–2023 period, following a long-term downward trend, similar to those observed in Bełchatów and the LGOM. A regular seasonal rhythm persists throughout the period. However, after 2015, the amplitude of fluctuations increased slightly, with more extreme positive and negative values. The 2019–2022 period is characterised by greater variability in CCDI. This suggests that local climatic conditions in Turów have become more unstable in recent years. The greater variability after 2015 may indicate more frequent periods of extreme conditions (e.g., more intense droughts interspersed with heavy rainfall).

### 6. Discussion and Conclusions

Given the pronounced drought conditions in open-pit mining areas, numerous studies have investigated the impacts of anthropogenic and climate-related factors. The levels of heavy metals associated with mining operations were examined. The susceptibility index ranged from 81 to 167, compared with 87 to 182 prior to mining operations. Heavy metals in soil adversely affect plant growth and pose environmental risks [33, 34]. Park et al. [35] analysed how a coal mine in Baganuur, Mongolia, contributes to soil pollution, dust emissions, and desertification. They noted that open-pit lignite mining processes degrade forests and grasslands.

**Table 5.** Comparison of parameters of the tested locations: Bełchatów, LGOM, Turów

Parameter	Bełchatów	LGOM	Turów
Long-term trend	declining (strong)	declining (moderate)	declining (clear)
Seasonality	strong, slightly decreasing after 2015	strong, stable	strong, with increasing amplitude after 2015
Data variability	high, especially 2003–2013	moderate, mild	increasing after 2015
Climate change direction	drying since 2018	more humid conditions	more variable, with greater extremes
Condition stability	relatively stable after 2015	very stable	less stable after 2015

Based on Table 5, a decline in CCDI values was observed in all analysed locations (Bełchatów, LGOM, and Turów) between 2003 and 2023, indicating a general long-term trend. Seasonality remains significant in each of the analysed mines, but local variability differs by region:

- LGOM – the most stable climate;
- Bełchatów – gradual weakening of seasonality;
- Turów – increasing variability and amplitude of change.

A significant drying trend has been observed since 2018. Further research is warranted, not only in open-pit mines but also in underground mining areas and other regions of Europe. Further research is warranted not only in open-pit mines but also in underground mining areas and other European regions. The period 2003–2009 was relatively stable, alternating dry and wet periods, consistent with the seasonal distribution in Poland. From late 2009 to 2015, conditions were generally wetter; notably, in 2010, Poland experienced a major flood that primarily affected the southern regions. Between 2015 and 2018, conditions stabilised again, but with increased amplitude of fluctuations between extremely dry and extremely wet states. After 2015, wet extremes became less frequent, while dry conditions intensified, particularly in 2018. As a result, wet periods largely disappeared, with values ranging mainly from normal to extremely dry.

### **Funding**

This research received no specific grant from any funding agency in the public, commercial, or not-for-profit sectors.

### **CRedit Author Contribution**

Z.R.: conceptualisation, methodology, software, validation, formal analysis, investigation, resources, data curation, writing – original draft preparation, writing – review and editing, visualisation, supervision, project administration, funding acquisition.

M.B.: conceptualisation, methodology, software, validation, formal analysis, investigation, resources, data curation, writing – original draft preparation, writing – review and editing, visualisation, project administration, funding acquisition.

### **Declaration of Competing Interests**

The authors declare that they have no known competing financial interests or personal relationships that could have appeared to influence the work reported in this paper.

### **Data Availability**

Data was acquired from:

- <https://hydro1.gesdisc.eosdis.nasa.gov/data/GLDAS/>, access: October 15, 2025.
- [https://hydro1.gesdisc.eosdis.nasa.gov/data/GLDAS/GLDAS\\_NOAH025\\_M.2.1/](https://hydro1.gesdisc.eosdis.nasa.gov/data/GLDAS/GLDAS_NOAH025_M.2.1/), access: October 15, 2025.

### **Use of Generative AI and AI-Assisted Technologies**

No generative AI or AI-assisted technologies were employed in the preparation of this manuscript.

## Appendix

The data used in the analysis can be organised as a matrix in which rows correspond to subsequent time epochs (253), and columns correspond to grid cells within the study area (1,125). For example, total water storage (TWS) values can be indexed as  $TWS[i, j]$ , where  $i = 1, \dots, 253; j = 1, \dots, 1,125$ . Let the indices of the grid cells corresponding to Bełchatów, LGOM, and Turów be denoted by  $j = j_B, j = j_L$ , and  $j = j_T$ . The quantities presented in Table 1 are then calculated as follows:

$$\text{– Mean over time Bełchatów: } \mu_T[j_B] = \frac{\sum_{i=1}^{253} TWS[i, j = j_B]}{253}$$

$$\text{– Mean over time LGOM: } \mu_T[j_L] = \frac{\sum_{i=1}^{253} TWS[i, j = j_L]}{253}$$

$$\text{– Mean over time Turów: } \mu_T[j_T] = \frac{\sum_{i=1}^{253} TWS[i, j = j_T]}{253}$$

$$\text{– Mean over time (max): } \max_j \{\mu_T[j]\}$$

$$\text{– Mean over time (min): } \min_j \{\mu_T[j]\}$$

$$\text{– Mean over time (overall): } \overline{\mu_T[j]}$$

$$\text{– Mean over cells (max): } \max_i \left\{ \mu_C[i] = \frac{\sum_{j=1}^{1,125} TWS[i, j]}{1,125} \right\}$$

$$\text{– Mean over cells (min): } \min_i \left\{ \mu_C[i] = \frac{\sum_{j=1}^{1,125} TWS[i, j]}{1,125} \right\}$$

$$\text{– Mean over cells (overall): } \overline{\mu_C[i]}$$

$$\text{– Max value: } \max_{i,j} \{TWS[i, j]\}$$

$$\text{– Min value: } \min_{i,j} \{TWS[i, j]\}$$

## References

- [1] Lian H., Yi H., Yang Y., Wu B., Wang R.: *Impact of coal mining on the moisture movement in a vadose zone in open-pit mine areas*. Sustainability, vol. 13(8), 2021, 4125. <https://doi.org/10.3390/su13084125>.
- [2] Haque E., Reza S., Ahmed R.: *Assessing the vulnerability of groundwater due to open pit coal mining using DRASTIC model: A case study of Phulbari coal mine, Bangladesh*. Geosciences Journal, vol. 22(2), 2017, pp. 289–301. <https://doi.org/10.1007/s12303-017-0054-0>.
- [3] Przybyłek J.: *Aktualne problemy odwadniania złóż węgla brunatnego w Wielkopolsce*. Górnictwo Odkrywkowe, r. 59(2), 2018, pp. 5–14.
- [4] Cui H., Duan L., Pan H., Zhang W., Liu T.: *How does large-scale underground mining affect the water cycle? Comprehensive analysis based on isotopes, water levels and hydrogeological conditions*. Journal of Environmental Management, vol. 393, 2025, 127188. <https://doi.org/10.1016/j.jenvman.2025.127188>.
- [5] Kraśnicki S.: *Report on the cross border effects of the continuation of lignite mining in Turów (Poland) on water in Germany*. September, 2022, [https://www.bund-sachsen.de/fileadmin/sachsen/Bilder/Mensch\\_\\_\\_Umwelt/Braunkohle/2023-Report\\_Turow\\_groundwater.pdf](https://www.bund-sachsen.de/fileadmin/sachsen/Bilder/Mensch___Umwelt/Braunkohle/2023-Report_Turow_groundwater.pdf) [access: October 15, 2025].
- [6] Bočková M.: *Twice about the Turów mine: Ministry responds to hydrogeological model, Supreme Administrative Court rejects miners' complaint*. Frank Bold, December 16, 2025. <https://en.frankbold.org/news/twice-about-the-turow-mine-ministry-responds-to-hydrogeological-model-supreme-administrative-court-rejects-miners-complaint> [access: October 15, 2025].
- [7] Wasilewski A., Rzepecka Z., Oszczak S.: *Studies of displacements of GPS stations on Polish copper basin area*, [in:] 10th FIG International Symposium on Deformation Measurements: Orange, California, USA, 19–22 March 2001, International Federation of Surveyors (FIG), 2001, pp. 223–231.
- [8] Chrzanowska A., Chrzanowski A., Oszczak S., Wasilewski A., Rzepecka Z., Popiołek E., Ostrowski J.: *Ocena przemieszczeń poziomych wyznaczonych technologią GPS i ich optymalne zastosowanie do analizy ruchów górotworu przy pomocy metody elementów skończonych (MES) dla terenów górniczych Rudna I i Rudna II*. Instytut Geodezji, Uniwersytet Warmińsko-Mazurski w Olsztynie, Olsztyn 1999.
- [9] *Protection of buildings in mining areas*. KGHM Polska Miedź. <https://kgbm.com/en/sustainable-development/environment/protection-buildings-mining-areas> [access: November 24, 2025].
- [10] *Kopalnia Węgla Brunatnego „Turów”*. Wikipedia: Wolna Encyklopedia. [https://pl.wikipedia.org/wiki/Kopalnia\\_Węgla\\_Brunatnego\\_„Turów”](https://pl.wikipedia.org/wiki/Kopalnia_Węgla_Brunatnego_„Turów”) [access: October 20, 2025].
- [11] *Czy węgiel brunatny to optymalny surowiec energetyczny dla Polski? Wbrew pozorom ma on swoje zalety*. Portal Statystyczny, May 26, 2021. <https://portalstatystyczny.pl/czy-wegiel-brunatny-to-optymalny-surowiec-energetycznym-dla-polski-wbrew-pozorom-ma-on-swoje-zalety/> [access: October 20, 2025].

- [12] *Kopalnia odkrywkowa węgla brunatnego Bełchatów*. Alol, July 7, 2021. <https://www.alol.pl/mapy/kopalnia-odkrywkowa-węgla-brunatnego-belchatow.html> [access: October 20, 2025].
- [13] *O oddziale*. PGE Górnictwo i Energetyka Konwencjonalna S.A. – Oddział Kopalnia Węgla Brunatnego Bełchatów. <https://kwbbelchatow.pgegielk.pl/O-oddziale> [access: October 20, 2025].
- [14] *Bełchatowski obszar węgla brunatnego. Co dalej z kopalnią Bełchatów?* Portal Statystyczny, October 20, 2022. <https://portalstatystyczny.pl/belchatowski-obszar-węgla-brunatnego-co-dalej-z-kopalnia-belchatow/> [access: October 20, 2025].
- [15] *Legnicko-Głogowski Okręg Miedziowy*. Wikipedia: Wolna Encyklopedia. [https://pl.wikipedia.org/wiki/Legnicko-Głogowski\\_Okręg\\_Miedziowy](https://pl.wikipedia.org/wiki/Legnicko-Głogowski_Okręg_Miedziowy) [access: October 20, 2025].
- [16] Oszczepalski S., Speczik S., Małecka K., Chmielewski A.: *Prospective copper resources in Poland*. *Gospodarka Surowcami Mineralnymi – Mineral Resources Management*, vol. 32(2), 2016, pp. 5–30. <https://doi.org/10.1515/gospo-2016-0019>.
- [17] Bartlett S.C., Burgess H., Damjanović B., Gowans R.M., Lattanzi C.R.: *Technical Report on the copper-silver production operations of KGHM Polska Miedź S.A. in the Legnica-Głogów Copper Belt area of southwestern Poland*. Micon International Limited, Norwich 2013. [https://kgm.com/sites/default/files/archive-attachments/raport\\_micon\\_en.pdf](https://kgm.com/sites/default/files/archive-attachments/raport_micon_en.pdf) [access: October 15, 2025].
- [18] Rodell M., Houser P., Jambor U.E.A., Gottschalck J., Mitchell K., Meng J., Arsenault K., Brian C., Radakovich J., Bosilovich M.G., Entin J.K., Walker J.P., Lohmann D., Toll D.L.: *The global land data assimilation system*. *Bulletin of the American Meteorological Society*, vol. 85(3), 2004, pp. 381–394. <https://doi.org/10.1175/BAMS-85-3-381>.
- [19] Rzepecka Z., Birylo M., Jarsjö J., Cao F., Pietroni J.: *Groundwater storage variations across climate zones from southern Poland to Arctic Sweden: Comparing GRACE-GLDAS models with well data*. *Remote Sensing*, vol. 16(12), 2024, 2104. <https://doi.org/10.3390/rs16122104>.
- [20] NASA Goddard Earth Sciences Data and Information Services Center (GES DISC) [dataset]. <https://hydro1.gesdisc.eosdis.nasa.gov/data/GLDAS/> [access: October 15, 2025].
- [21] NASA Goddard Earth Sciences Data and Information Services Center (GES DISC) [dataset]. [https://hydro1.gesdisc.eosdis.nasa.gov/data/GLDAS/GLDAS\\_NOAH025\\_M.2.1/](https://hydro1.gesdisc.eosdis.nasa.gov/data/GLDAS/GLDAS_NOAH025_M.2.1/) [access: October 15, 2025].
- [22] Rzepecka Z., Birylo M., Kuczynska-Siehien J., Nastula J., Pajak K.: *Analysis of groundwater level variations and water balance in the area of the Sudety mountains*. *Acta Geodynamica et Geomaterialia*, vol. 14(3), 2017, pp. 313–321. <https://doi.org/10.13168/AGG.2017.0014>.
- [23] Rahgozar M., Shah N., Ross M.: *Estimation of evapotranspiration and water budget components using concurrent soil moisture and water table monitoring*. *ISRN Soil Science*, vol. 2012, 726806. <https://doi.org/10.5402/2012/726806>.

- [24] Lu Z., Li K., Zhang J., Le G., Yu Z., Li C.: *Mechanisms influencing changes in water cycle processes in the changing environment of the Songnen Plain, China*. Science of The Total Environment, vol. 905, 2023, 166916. <https://doi.org/10.1016/j.scitotenv.2023.166916>.
- [25] Birylo M., Rzepecka Z.: *Remote sensing-based hydro-extremes assessment techniques for small area case study (the case study of Poland)*. Remote Sensing, vol. 15(21), 2023, 5226. <https://doi.org/10.3390/rs15215226>.
- [26] Sinha D., Sayed T.H., Reager J.: *Utilizing combined deviation of precipitation and GRACE based terrestrial water storage as a metric for drought characterization: A case study over major Indian river basin*. Journal of Hydrology, vol. 572, 2019, pp. 40–50. <https://doi.org/10.1016/j.jhydrol.2019.02.052>.
- [27] Nigatu Z.M., Fan D., You W., Melesse A.M.: *Hydroclimatic extremes evaluation using GRACE/GRACE-FO and multidecadal climatic variables over the Nile River Basin*. Remote Sensing, vol. 13(4), 2021, 651. <https://doi.org/10.3390/rs13040651>.
- [28] Rzepecka Z., Birylo M., Nastula J.: *Assessment of resultant groundwater calculated on the basis of GRACE and GLDAS models*, [in:] *16th International Multidisciplinary Scientific GeoConference (SGEM 2016): Albena, Bulgaria, 30 June–6 July 2016. Book 2, Volume 2, Part A: Geodesy and Mine Surveying*, Curran Associates, Red Hook 2016, pp. 125–132.
- [29] Birylo M.: *Non-stationarity of hydroclimatic memory – is hydrological memory changing under climate warming?* Water, vol. 18(7), 2026, 869. <https://doi.org/10.3390/w18070869>.
- [30] Birylo M., Blaszczyk-Bak W., Suchocki C.: *Application of GLDAS models and ALS point clouds in assessing the impact of modified evapotranspiration on the water budget*. Water Research, vol. 283, 2025, 123746. <https://doi.org/10.1016/j.watres.2025.123746>.
- [31] Meals D.W., Spooner J., Dressing J.A., Harcum J.B.: *Statistical analysis for monotonic trends*. Tech Notes, no. 6, Tetra Tech, Fairfax, VA, 2011. <https://www.epa.gov/polluted-runoff-nonpoint-source-pollution/nonpoint-source-monitoring-technical-notes> [access: June 23, 2025]
- [32] Hipel K.W., McLeod A.I.: *Time Series Modelling of Water Resources and Environmental Systems*. Developments in Water Science, vol. 45, Elsevier, 1994.
- [33] Wierzbowska J., Sienkiewicz S., Krzebietka S., Bowszys T.: *Heavy metals in water percolating through soil fertilized with biodegradable waste materials*. Water, Air, & Soil Pollution, vol. 227(12), 2016, 456. <https://doi.org/10.1007/s11270-016-3147-x>.
- [34] Wierzbowska J., Kovacik P., Sienkiewicz S., Krzebietka S.: *Determination of heavy metals and their availability to plants in soil fertilized with different waste most stable conditionsances*. Environmental Monitoring and Assessment, vol. 190(10), 2018, 567. <https://doi.org/10.1007/s10661-018-6941-7>.
- [35] Park J., Kwon E., Chung E., Kim H., Battogtokh B., Woo N.C.: *Environmental sustainability of open-pit coal mining practices at Baganuur, Mongolia*. Sustainability, vol. 12(1), 2020, 248. <https://doi.org/10.3390/su12010248>.